Duquesne Light Company

Beaver Valley Power Station
P.O. Box 4
Shippingport, PA 15077-0004
(412) 393-5206
(412) 643-8069 FAX

GEORGE S. THOMAS
Division Vice President
Nuclear Services
Nuclear Power Division

July 9, 1993

U. S. Nuclear Regulatory Commission
Attn: Document Control Desk
Washington, DC 20555

Subject: Beaver Valley Power Station, Unit No. 1
BV-1 Docket No. 50-334, License No. DPR-66
Response to Information Request Dated June 8, 1993
Spent Fuel Pool Rerack
(TAC No. M84673)

This letter provides a response to your request for additional information regarding our proposed Technical Specification Change Request No. 202, submitted by letter dated November 2, 1992. These concerns are related to the seismic analyses that were performed to rerack the spent fuel pool. Attachment A provides each item followed by our response.

If you have any questions regarding the attached response, please contact Mr. Steve Sovick at (412) 393-5211.

Sincerely,

George S. Thomas

Attachment

cc: Mr. L. W. Rossbach, Sr. Resident Inspector
Mr. T. T. Martin, NRC Region I Administrator
Mr. G. E. Edison, Project Manager
Mr. M. L. Bowling (VEPCO)

150011

A001 1/1

Beaver Valley Power Station, Unit No. 1
Response to Information Request Dated June 8, 1993
Spent Fuel Pool Rerack

ATTACHMENT A

Item 1

On page 6-9 it is stated that, "In the fuel rack simulations, the coulomb friction interface between rack support pedestal and liner is typical of a nonlinear spring." Please state the mathematical formulation of this nonlinear spring and describe the physical meaning of this formulation.

Response 1

Coulomb friction force at a point is defined as:

$$F \leq \mu N$$

where N is the normal force on the friction interface, μ is the coefficient-of-friction, and F is the supportable lateral force available from friction. The Coulomb friction force is reactive, rather than active. In other words, it develops only to counteract a laterally applied external force and its value cannot exceed the lesser of μN or the applied external force, P; i.e., referring to Figure 1A: at any instant of time, the friction force is the minimum of either P or μN. In DYNARACK, the FORTRAN definition is:

F = AMIN [P, μN] where AMIN is the minimum friction force on body A and P and N are absolute values. The direction of F is such as to oppose the direction of actual or impending motion.

It therefore follows for this simple example, that the body A subject to given interface load N, will begin to slide if the lateral load exceeds μN and the lateral displacement, δ, of body A will have the relationship depicted by Figure 1B, which can be written symbolically as:

$$\delta = 0 \text{ if } P \leq \mu N$$
$$= \infty \text{ if } P > \mu N$$

δ can be viewed as the slip between the point 0' and 0 at the friction interface in Figure 1.

Response 1 (Continued)

The "ideal" Coulomb friction force-displacement profile shown in Figure 1B can be written in the more generalized form (refer to Figure 1C) as:

$$F = \text{AMIN}\,[P, K\delta], \text{ if } K\delta < \mu N, \dot{\delta} \approx 0$$

$$= \text{AMIN}\,[P, \mu N]; \text{ if } K\delta > \mu N, \dot{\delta} \approx 0$$

where K is the stiffness of the theoretical spring connecting point 0 and 0' at the interface in Figure 1A. Reference [6.4.4] of the submittal states that the spring constant, K, should be chosen an order of magnitude larger than the characteristic elastic stiffness of the interface structure.

The relationship exhibited by the above formula is the Coulomb piecewise linear spring utilized in DYNARACK. It is a standard procedure in numerical simulation of friction interfaces and is succinctly described in the reference [6.4.4, pages 29 and 30]. The methodology is also routinely used in Finite Element Codes such as ANSYS[1] where the CONTACT26 element offers friction capabilities.

Item 2

On page 6-10 it is stated that, "The fuel rack structure is very rigid." What is the fundamental frequency of the rack?

Response 2

The spent fuel racks are free-standing structures and therefore are capable of undergoing rigid body motions. In addition, they will undergo elastic motions which are superposed on the gross rigid body motions. DYNARACK incorporates this elastic motion of the rack cellular structure by considering the cantilever beam action, in two directions, of the cellular structure with respect to the baseplate. The calculated elastic beam frequency corresponding to the elastic deflection shape is high, compared to the predominant frequency of the input seismic motions. For the 11 x 15 spent fuel rack (weight = 24,300 lbs), the moment of inertia in the weakest direction is

---

1 ANSYS Rev. 5.0, Vol. III, Thecretical Manual, 1992.

Response 2 (Continued)

computed and the lowest cantilever beam frequency calculated as 69.9 HZ if we consider only the mass of the spent fuel rack in the frequency calculation. In the actual analyses, the fuel moves separately (horizontally) from the spent fuel rack. Notwithstanding this, if we conservatively assume that the rack is fully loaded with fuel assemblies of weight 1600 lbs per assembly, and that these assemblies are attached to the rack at all times, then the calculated lowest natural frequency drops to 20.3 HZ. This is a lower bound but is nevertheless still much higher than the predominate seismic input frequencies which are on the order of 5-7 HZ.

Item 3

On page 6-11 it is stated that, "Fluid coupling between rack and fuel assemblies, and between rack and wall, is simulated by appropriate inertial coupling in the system kinetic energy." Provide sketches to indicate the physical model of the inertial coupling and describe how the model was represented mathematically.

Response 3

Hydrodynamic forces occur between fuel assemblies and fuel cell walls, and on a larger scale between adjacent racks and/or between racks and walls. The hydrodynamic effect occurs as the relatively small gaps between racks in a maximum density configuration are squeezed and opened by the movement of adjacent racks during a seismic event.

To understand the nature of the forces arising due to hydrodynamic mass coupling, consider Figure 2 which shows two plates, forming a narrow fluid channel, approaching one another with speed u. The moving planes, for simplicity, are assumed infinitely long such that the motion of water exiting the inter-plane space remains in the plane of the paper. For this geometry, the average velocity of the exiting fluid ρ is computed by a direct volume balance. In the time interval Dt

$$W(2u)Dt = 2\rho d(Dt)$$

or

$$\rho = U \frac{W}{d}$$

Response 3 (Continued)

The conclusion is that the speed of the water exiting the gap is W/d times the approach speed of the plane. In a typical maximum density spent fuel pool configuration, the ratio W/d is of the order 50-100. Since kinetic energy is proportional to the square of the speed, the water exiting the inter-rack space may have as much as 2500-10,000 times the specific kinetic energy of the rack. This hydraulic energy is either drawn from or added to the moving rack and modifies the rack submerged motion in a significant manner. In the maximum density configurations now in use, this effect cannot be neglected or approximated (note that for earlier low density rack configurations wide fluid gaps enabled arguments leading to consideration of the hydrodynamic effect only as it added mass to the rack). The above simple model illustrates the significance of hydrodynamic mass consideration in spent fuel rack seismic analyses.

To extend this simplest technology to a spent fuel pool in a maximum density configuration, consider Figure 3 which shows a "center rack" C surrounded by eight adjacent racks. The fluid gaps 1...4 shown on the figure are between rack C and racks R, T, L and B, respectively. The presence of fluid effectively means that all racks in the pool are coupled in their dynamic response. Thus, without further simplifying assumptions, all racks in the pool should be considered for dynamic simulations. For example, a single rack analysis of rack C, is performed by assuming that racks R, T, L and B move either completely out-of-phase with rack C, or by assuming that they move totally in-phase with rack C. In either case, racks TR, TL, BL, BR are assumed to have no fluid coupling with rack C. The simplest gap squeezing model assumes that the fluid in gap 1 is affected only by the motion of racks C and R and exhausts into an infinite reservoir. Similar assumptions hold for gaps 2, 3 and 4. That is, the hydrodynamic mass contribution in any gap depends only on the movement of adjacent racks, and the fluid squeezed out, for example, does not necessarily travel around the rack. In other words, the fluid motion in any gap is assumed to behave as if each separate gap exhausted into an infinite reservoir.

Figures 4 and 5 illustrate the concept of in-phase and out-of-phase motion of adjacent racks as applied to a detailed analysis of single rack C. U and V in Figures 4 and 5 are the displacements of the rack. In Figure 4, the equations governing the behavior of the single rack C exhibit minimal fluid coupling. In the case illustrated by Figure 5, the equations governing the behavior of rack C will contain a strong fluid coupling effect which will involve only the C rack velocity by virtue of the out-of-phase assumption. In either case, the assumptions on adjacent rack behavior are what decouples the problem down to a single rack analysis.

Response 3 (Continued)

The above discussion focused on a single rack chosen from the total number in the pool. Based on an assumed motion of adjacent racks, a hydrodynamic contribution can be assessed which will involve only the rack being analyzed. This approach constituted the "state of the art" in spent fuel pool reracking efforts until recently (ca. 1988), and allows complete decoupling of the rack being analyzed from adjacent racks. Despite the versatility of a 3-D seismic model, analyzed by direct time integration, the accuracy of the simulations has been suspect due to the unknown effect of the hydrodynamic decoupling assumption. Given the fact that the presence of the fluid causes the dynamics of one rack to affect the motion of all other racks in the pool, especially for closely spaced racks, a dynamic simulation which treats only one rack or only a small sub-set of racks, may be intrinsically inadequate to predict the motion of the full array of rack modules to an acceptable level of confidence. The only way to be sure is to consider all racks in the pool, make no assumptions on rack behavior, and let the solution dictate what really happens. The mathematical theory for the whole pool simulation has been developed and incorporates the effects of whole pool fluid dynamics. The development requires no more than fundamental fluid mechanics concepts applied to a geometry consisting of an array of channels.

Item 4

On page 6-11 it is stated that, "Potential impacts between rack and fuel assemblies are accounted for by appropriate compression-only gap elements between masses involved." Please illustrate how the gap elements actually accounts for the potential impacts between the rack and fuel assemblies (use sketches and description).

Response 4

Figure 6 shows two masses separated by a compression-only gap element. G is the initial gap, ≥ 0, between the two masses. The mass motion is described by variables $U_1(t)$ and $U_2(t)$. The spring constant K reflects the local stiffness between the two masses. Figure 7 shows the force deflection relationship for the compression-only gap element. During the motion, if U_1-U_2 is less than the initial gap prescribed, the masses are not in contact and the force in the gap element is zero. If the gap closes, then $U_1-U_2-G > 0$, and a force builds up in accordance with the local stiffness K. When the gap opens, at some other time, then the force drops to zero. In DYNARACK, the status of each gap element is checked at each instant during the solution, and the equilibrium equations updated to reflect open or closed gaps.

Item 5

On page 6-11 it is stated that, "Local pedestal spring stiffness accounts for floor elasticity and for local rack elasticity just above the pedestal." Describe the mathematical formulation of the local pedestal spring stiffness in general, and of the floor elasticity and local rack elasticity in particular.

Response 5

The pedestal spring modeling the vertical stiffness of the floor-pedestal-rack structure is a gap element at each pedestal location. The overall stiffness value ascribed is obtained by considering the serial effect of each of the contributing factors. The major effects are due to the pedestal stiffness, the stiffness of the local structure under the pedestal, and the local stiffness of the cellular structure in the immediate vicinity of a pedestal. The equation is:

$$\frac{1}{K_s} = \frac{1}{K_1} + \frac{1}{K_2} + \frac{1}{K_3}$$

where K_s is the effective stiffness of the ensemble, K_1 is the spring rate of the pedestal metal structure considered as an axial tension compression member, K_2 is the local spring rate of the pool slab, and K_3 is the local spring rate of the folded plate structure above the particular support leg. K_2 is obtained by using [6.4.4], which contains formulas for pads in contact with halfspaces; and K_3 is obtained from the classical solution for a point load on a semi-infinite quarter space. The Young's Modulus used in the determination of K_3 is reduced to reflect the fact that the "space" is a gridwork rather than a solid homogenous material. The final value for K_s is influenced most heavily by the value of K_3 which generally is smaller than K_1 or K_2.

Item 6

On page 6-13 it is stated that rack-to-rack gap elements can be found in Figure 6.4.3. However, the title of Figure 6.4.3 is "rack-to-rack impact springs" and the designation of the springs in the Figure is labeled as "typical impact element." Are "gap element" and "impact spring" and "impact element" the same thing?

Response 6

Yes. The terminology "gap element," "impact spring," and "impact element" refer to the same entity; namely, the compression-only elements already discussed in responses 4 and 5.

Item 7

Table 6.4.2 contains numbering system for gap elements and friction elements. Provide a drawing of the model that shows the gap and friction elements as stated in Table 6.4.2.

Response 7

Figures 8A and 8B provide multiple view drawings for clarity.

Item 8

On page 6-16 it is stated that, "It is noted that sliding will occur at the pedestal-bearing pad interface before it occurs at the bearing pad-liner interface. This can be assured by the use of dissimilar material constitution between pedestal and pad, whereas the same material constitution is used in the bearing pad and liner." Do the analysis results in Beaver Valley show that any bearing pad slides against the linear? If not in this case, could it happen in other cases where seismic movements are relatively higher than this case?

Response 8

The analyses performed for Beaver Valley indicate that no bearing pad sliding, relative to the liner, will occur. This conclusion is site specific and depends on rack parameters, loading, and site seismic loading. Therefore, it cannot be stated categorically that bearing pad/liner sliding will never occur if seismic inputs (and resulting movements) are higher.

Item 9

On page 6-22 it is stated that, "Stress results are presented in dimensionless form. Dimensionless stress factors are defined as the ratio of the actual developed stress to the specified limiting value. Stress factors are only developed for the single rack analyses. The limiting value of each stress factor is 1.0 for OBE and 2.0 (or less) for the SSE condition." Provide reasons to justify the criterion which allows the limiting value of stress factors exceeding 1.0 or the actual stress exceeding the specified limiting value.

Response 9

Section 6.5.2 of the submittal provides stress limits for all conditions except faulted conditions. The limits are in accordance with ASME, Section III, Subsection NF. Section 6.5.2.2 provides the Code rule for dealing with faulted (SSE) conditions. The Code rules are designed to limit primary stresses acting on the gross cross section; no limits are set on secondary stresses. Primary stresses are not self-limiting, are caused by externally applied mechanical loads, and are required to be in equilibrium with the external loads. Secondary stresses, on the other hand, arise solely to satisfy compatibility, are self-limiting, and are not needed to satisfy equilibrium. Stress limits, for other than "faulted" events, are set to ensure that primary stresses remain well below the material yield stress. For "faulted" events (the Level D condition), the Code sets the elastically computed primary stress limit to be the lesser of 1.2 x yield stress or 0.7 x ultimate stress. Essentially, this means that during a faulted condition event, portions of a cross section under bending may undergo some yielding, but the gross cross section will not experience a total moment in excess of that needed to maintain equilibrium. Essentially the Code recognizes that after a Level D event, there may be some small localized permanent deformation, but that component safety will not be compromised.

Notwithstanding the limits permitted by the Code, for Beaver Valley new spent fuel racks, the computed stress factors demonstrate that even for Level D conditions, the primary stresses under all designated combinations, remain in the elastic range.

Item 10

On page 6-27 it is stated that, "Local cell wall integrity is conservatively estimated from peak impact loads. Plastic analysis is used to obtain the limiting impact load." Should the word "limiting" be replaced by "peak"? Describe the procedures of this plastic analysis that were used to obtain the limiting, or peak, impact load.

Response 10

No, the words are correct as used. The peak impact loads are determined from the results of the actual seismic event. Plastic (or limit) analysis is used to compute the limiting impact load which can be sustained without undergoing permanent deformations which could compromise safety. The peak impact load must be less than the calculated limiting impact load.

Response 10 (Continued)

The limiting impact load that can be supported is determined by modeling a strip of cell wall which is in contact (during an impact) with the fuel assembly at a given location. The limiting impact load is that load which when exceeded will lead to large deformations under any further increase in load. Figure 9 sequentially shows the calculation applied to a clamped beam under a uniform load. The factor p_c times the length of the beam is the collapse load in this case, p_cL must be greater than the corresponding peak load calculated from the dynamic event. Figure 9 shows the configuration for a uniformly loaded strip for illustrative purposes only; the limit load calculation for fuel assembly-cell wall impact is based on two concentrated forces applied to the beam strip at the fuel cell/fuel assembly contact locations subsequent to the impact.

Item 11

On page 6-28 it is stated that, "This upper bound value is obtained by using the highest rack-to-fuel impact load from Table 6.7.5 (for any simulation), and multiplying the result by 2 (assuming that two impact locations are supported by every weld connection). Justify the assumption that the two impact locations are supported by every weld connection.

Response 11

The spent fuel/fuel rack model in DYNARACK separates the fuel assembly into five discrete masses which are equally spaced along the assembly length. The low flexural stiffness of a fuel assembly and the fluid force contribution of the water ensure that the assembly will undergo various curved contours, and the rattling impacts will likely occur both at grid strap and non-grid strap locations. Holtec's assumption of five impact locations, thus concentrating the impact load, ensures that the peak values of these calculated loads will be higher than what may actually occur at any point.

There are six welded connecting bars along the height, one at the bottom of the rack, one at the top, and four equally spaced between top and bottom. This ensures that each modeled impact location is, at worst, between two weld bar locations.

To ensure load transfer capability, the highest peak impact load is chosen and then multiplied by 2 so as to disregard any phase effects between impact loads (which would tend to decrease the sum). In summary, the analysis for the connecting welds is conservative because it uses a peak dynamic load for comparison purposes, and uses a design load that disregards the reducing effects of impact load phasing. Even with this conservatism in the calculation of the load, Table 6.7.42 shows that there is a safety margin of almost 9 against weld overstress due to excessive load.

Item 12

On page 3-1 it is stated that, "The storage cells are connected to each other by austenitic stainless steel corner welds which leads to a honeycomb lattice construction. The extent of welding is selected to "detune" the racks from the seismic input motion (OBE, and SSE)." Explain how the welding was selected to detune the racks from the seismic input motion.

Response 12

The extent of cell-to-cell corner welds is optimized from both fabrication and structural standpoints. Stainless steel in gage stock is highly prone to weld induced distortion. Maintaining an extremely tight fabricational tolerance is a key requirement in fuel rack fabrication. The other design imperative is to ensure that the rack modules undergo minimal displacements during the postulated governing seismic event. While the notion of "resonance" is germane only to linear structures, non-linear systems such as spent fuel racks do exhibit some dependence on the structural stiffness of the module. The most direct means to adjust the stiffness matrix is through the extent of cell-to-cell connectivity to minimize weld induced distortions as well as the maximax (maximum in time and space) displacements. Fortunately for typical rack conditions, the optimum design, the so-called detuned configuration, meets the above-mentioned fabrication objectives as well.

The procedure followed involves considering a model of an isolated rack (to minimize fluid coupling effects), subjecting the configuration to a 3-D event, and varying the effects of varying cell-to-cell connectivity. This effect primarily influences the structural inertia properties of the rack. The effect of the detuning simulations on response is evaluated and the extent of welding established consistent with both fabrication and analysis objectives.

Item 13

What are the clearances between the racks during plant operation? Describe inspection procedures for fuel racks after being subjected to OBE level earthquakes and corrective procedures for those racks which have been moved or shifted as a result of earthquakes.

Response 13

Design clearances between racks are 3/4" between any Region II racks, 1-3/4" between any Region I and Region II racks, and 2" between the Region I racks. The geometry of the racks is such as to ensure that the "as-installed" minimal gaps maintain radiological, structural, and thermal hydraulic safety margins. For example, rack baseplate extensions beyond the cellular regions ensure that the 2" Region I to Region I gap is maintained. As-installed gaps are measured and archived after completion of rack installation. Subsequent to an OBE event, we plan to measure inter-rack and rack-to-wall gaps at pre-selected control locations. In the event that the control location gaps differ from the as-installed gaps, we will either analytically evaluate and demonstrate (if feasible) the continued acceptability of the altered configuration or take applicable steps to restore the gaps to original values (within $\pm$ 1/8" tolerance). A safety evaluation in accordance with 10 CFR 50.59 will be developed to verify that safety criteria are maintained.

Item 14

The nonlinear computer program DYNARACK has been used to analyze the rack responses during earthquakes. Has the program been validated against test data from free standing racks emerged in the water and subjected to seismic loads, if any? As applicable, discuss the extent and key features of the verification and justify that the types of verification implemented would assure obtaining of correct results from nonlinear DYNARACK analysis.

Response 14

DYNARACK has not been validated against test data from full size free-standing racks immersed in water and subject to seismic loads.

The experimental verification of DYNARACK done to date had to be performed on a scaled model since full scale testing would involve very large inertia, fluid, and friction forces which would outstrip the capability of calibrated testing in any U.S. laboratory. To our knowledge, the only effort at full scale testing was in Japan, which, too, falls short of the objective because some key loadings such as the fluid coupling forces, were eliminated from the experiment, presumably to keep the testing effort manageable. The Japanese data is incomplete and unavailable to us.

Response 14 (Continued)

Holtec's scaled model testing focused on the two key contributors to the dynamics of the racks - the fluid coupling and the inertia forces. The results from almost 100 experiments demonstrated remarkable agreement between the predictions of the DYNARACK Code and the experimental data.

The complete verification of DYNARACK involves not only the experimental work discussed above but also an extensive set of analytical simulations.

A validation manual for DYNARACK has been previously submitted to the USNRC on two dockets (TMI Unit One and D.C. Cook). A brief outline of the validation is provided in the following.

The validation of DYNARACK is in conformance with the provisions of the Holtec Quality Procedure HQP 5.2, Computer Programs, and demonstrates that DYNARACK meets all validation requirements of USNRC-SRP 3.8.1. Section II.4(e) of SRP 3.8.1 states that computer programs used in design and analysis should be described and validated by any of the following procedures or criteria:

(i) The computer program is a recognized program in the public domain, and has had sufficient history of use to justify its applicability and validity without further demonstration.

(ii) The computer program solution to a series of test problems has been demonstrated to be substantially identical to those obtained by a similar and independently written and recognized program in the public domain. The test problems should be demonstrated to be similar to or within the range of applicability of the problems analyzed by the public domain computer program.

(iii) The computer program solution to a series of test problems has been demonstrated to be substantially identical to those obtained from classical solutions or from accepted experimental tests, or to analytical results published in technical literature. The test problems should be demonstrated to be similar to or within the range of applicability of the classical problems analyzed to justify acceptance of the program. A summary comparison should be provided for the results obtained in the validation of each computer program.

Since DYNARACK is a private domain program, the validation problems used for DYNARACK comply with criteria (ii) and (iii) above.

Response 14 (Continued)

In the DYNARACK Validation Report, it is shown that DYNARACK meets the following criteria:

1. All desired capabilities of the code perform as expected.

2. Results from DYNARACK are in excellent agreement with solutions obtained from other sources.

3. The fluid coupling methodology in DYNARACK is demonstrated to be in agreement with experimental results.

4. The code exhibits excellent convergence when applied to both linear and nonlinear problems.

In summary, DYNARACK has been benchmarked against a wide array of linear and nonlinear problems in dynamics which have been chosen to test the veracity of every type of element which has been incorporated into the spent fuel rack model.

The experimental validations have reinforced the veracity of the hydrodynamic coupling theory used in DYNARACK.

To our knowledge, DYNARACK is the only code used for spent fuel racks with such a complete underlay of validations. To our knowledge, no other simulation code is available which contains a validated hydrodynamic coupling methodology suitable for modeling the effects of an entire fuel pool.

Beaver Valley Power Station, Unit No. 1
Response to Information Request Dated June 8, 1993
Spent Fuel Pool Rerack

FIGURES 1 THROUGH 9

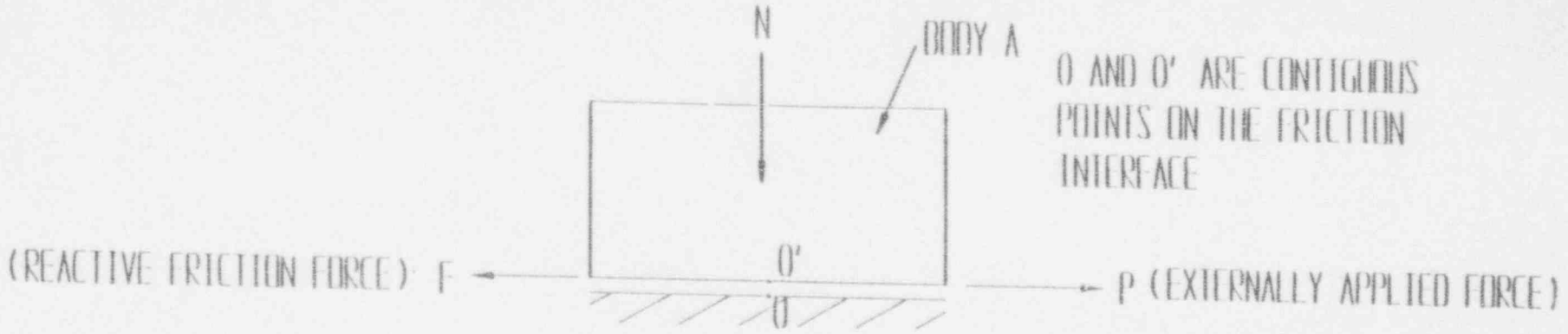

FIGURE 1A

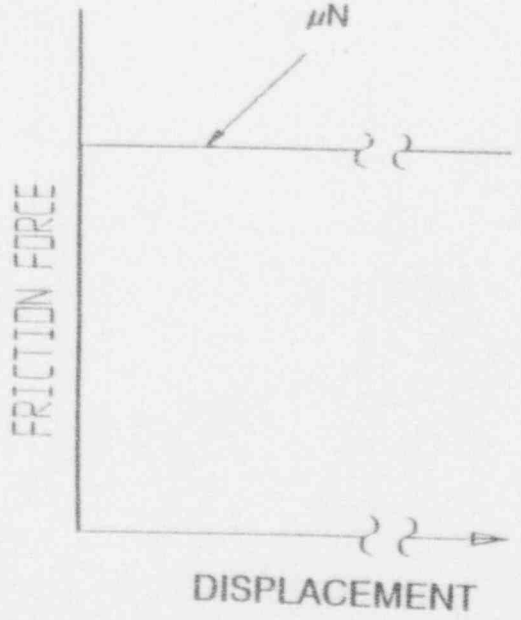

FIGURE 1B

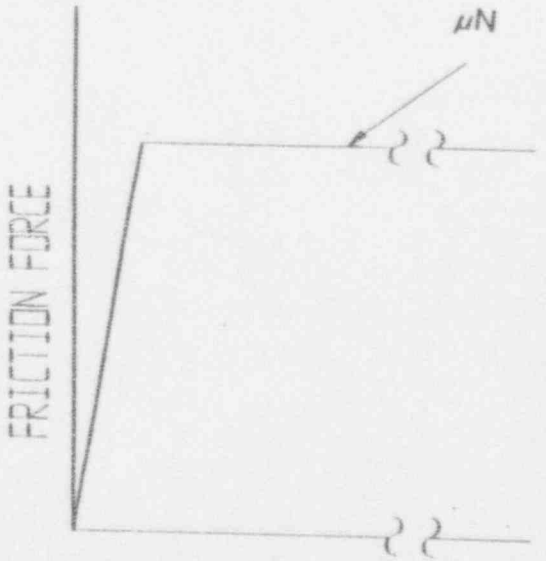

FIGURE 1C

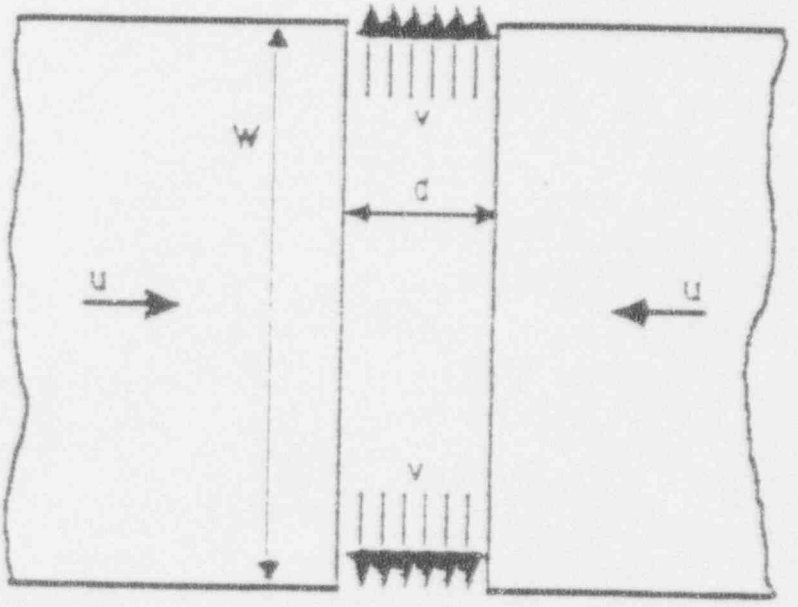

FIGURE 2 HYDRODYNAMIC EFFECT BETWEEN TWO PLATES

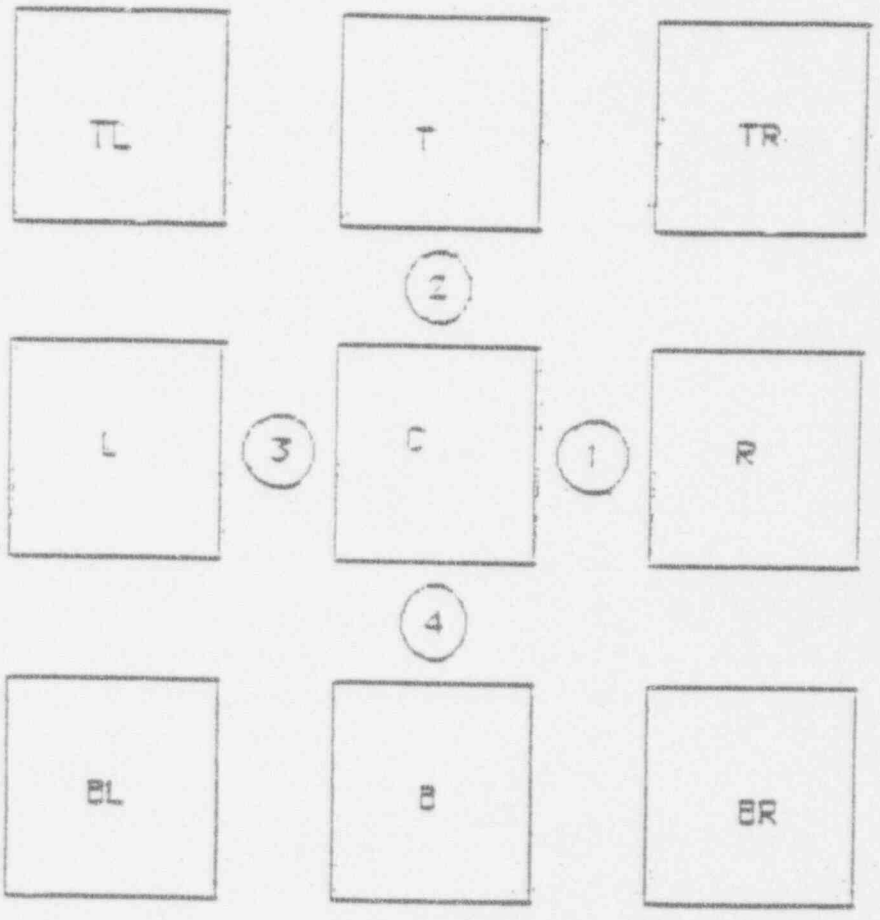

FIGURE 3 HYDRODYNAMIC COUPLING IN RACK ARRAY

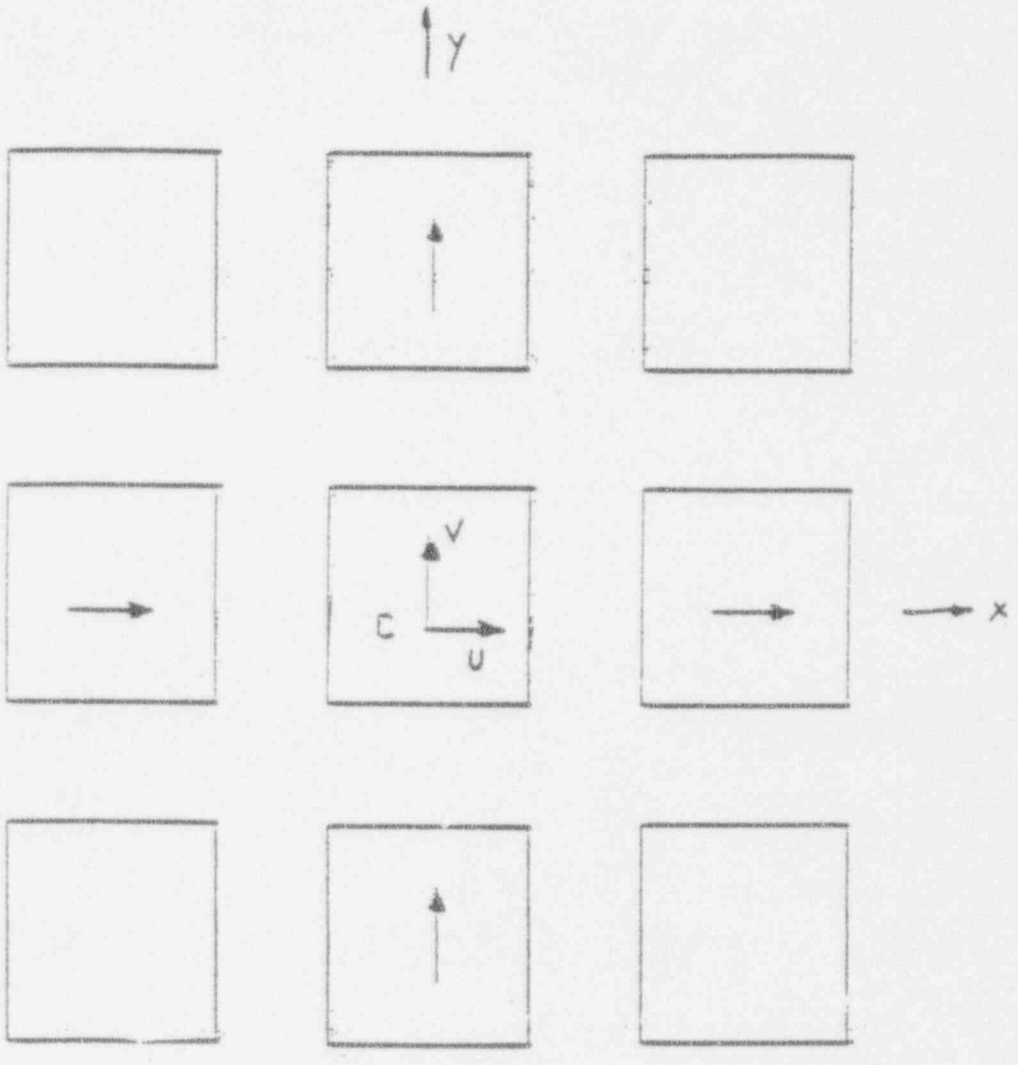

FIGURE 4 IN-PHASE RACK MOTION (NO GAP SQUEEZING)

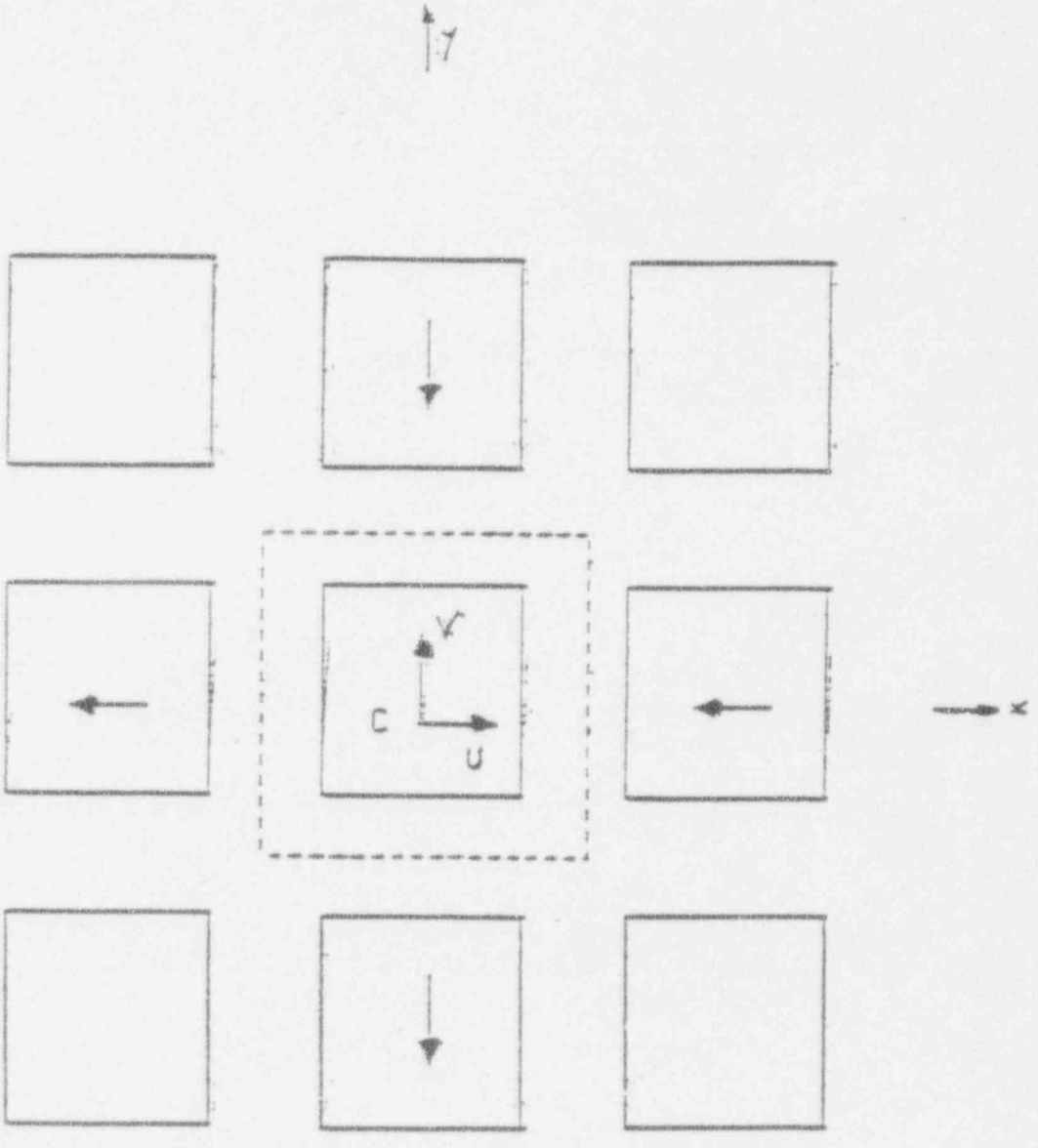

FIGURE 5 OUT-OF-PHASE MOTION

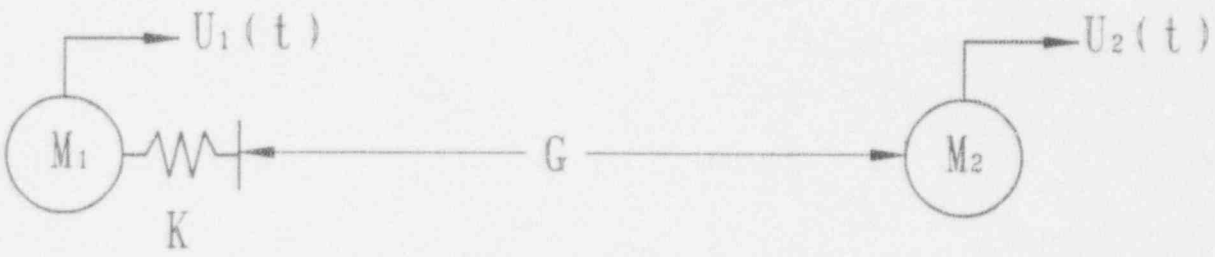

FIGURE 6

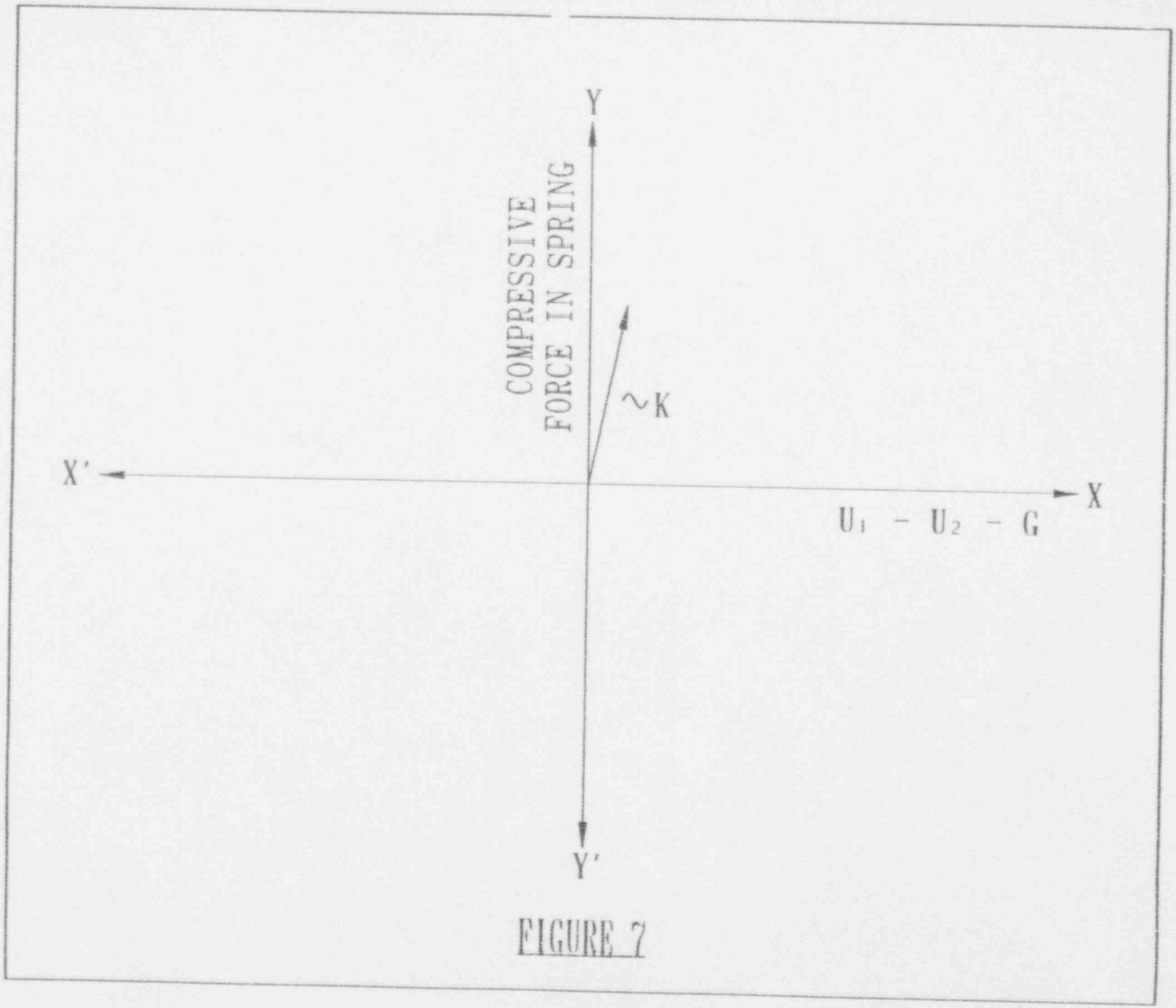

FIGURE 7

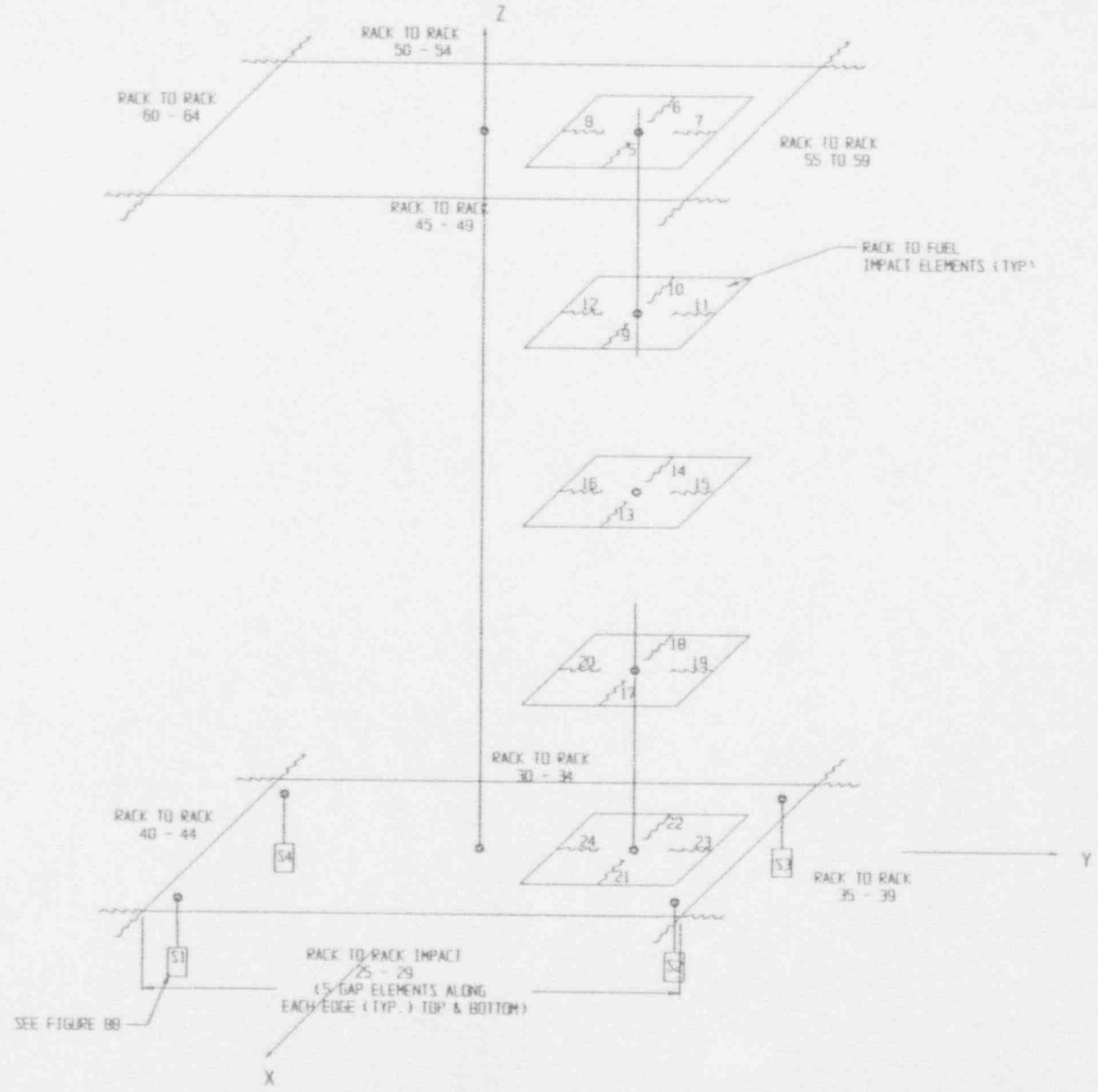

FIGURE - 8A DYNARACK NONLINEAR ELEMENTS
(ELEMENT NUMBERS REFER TO TABLE IN SUBMITTAL)

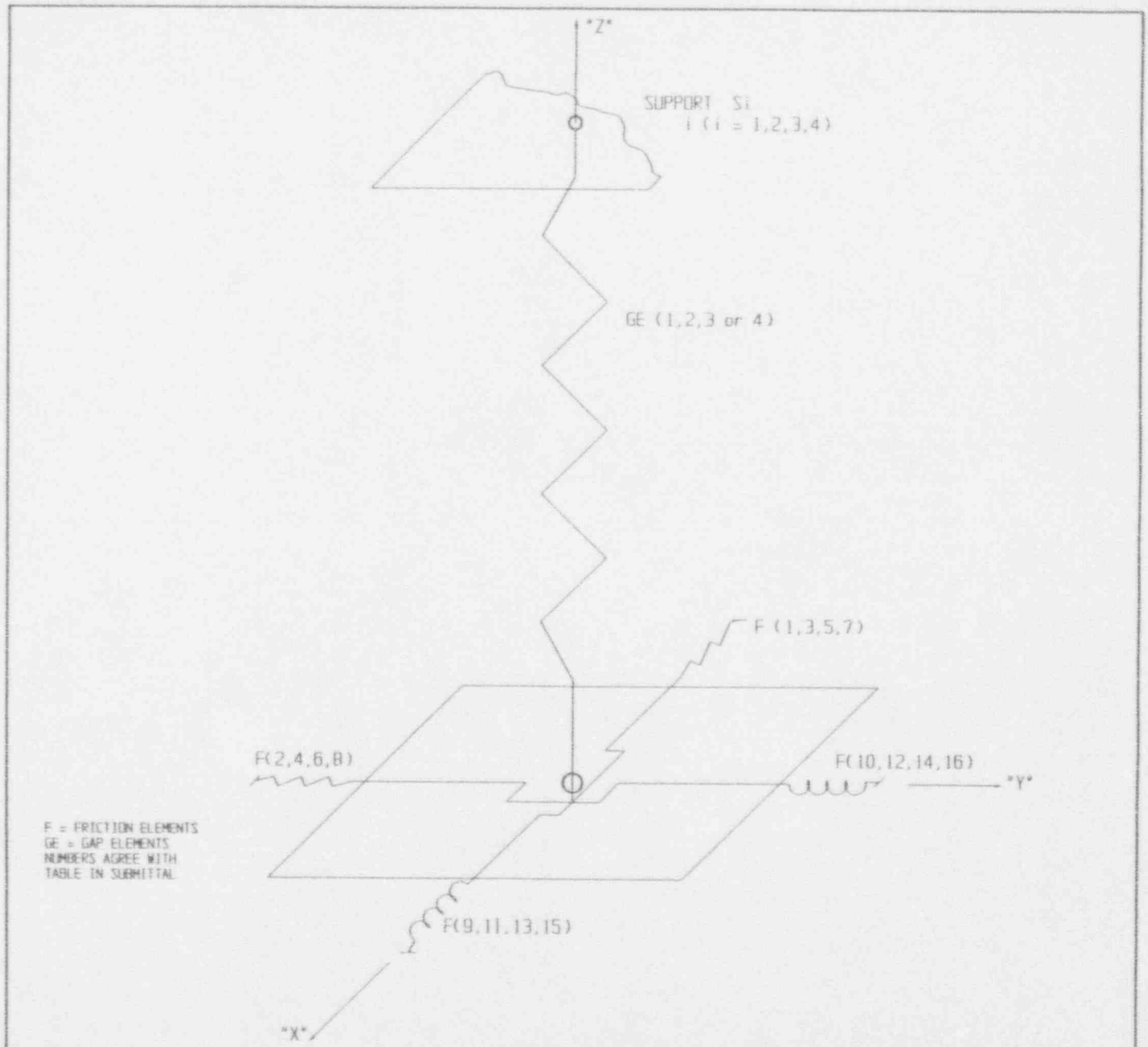

FIGURE - 8B
DETAIL SHOWING GAP AND FRICTION ELEMENTS AT SUPPORT

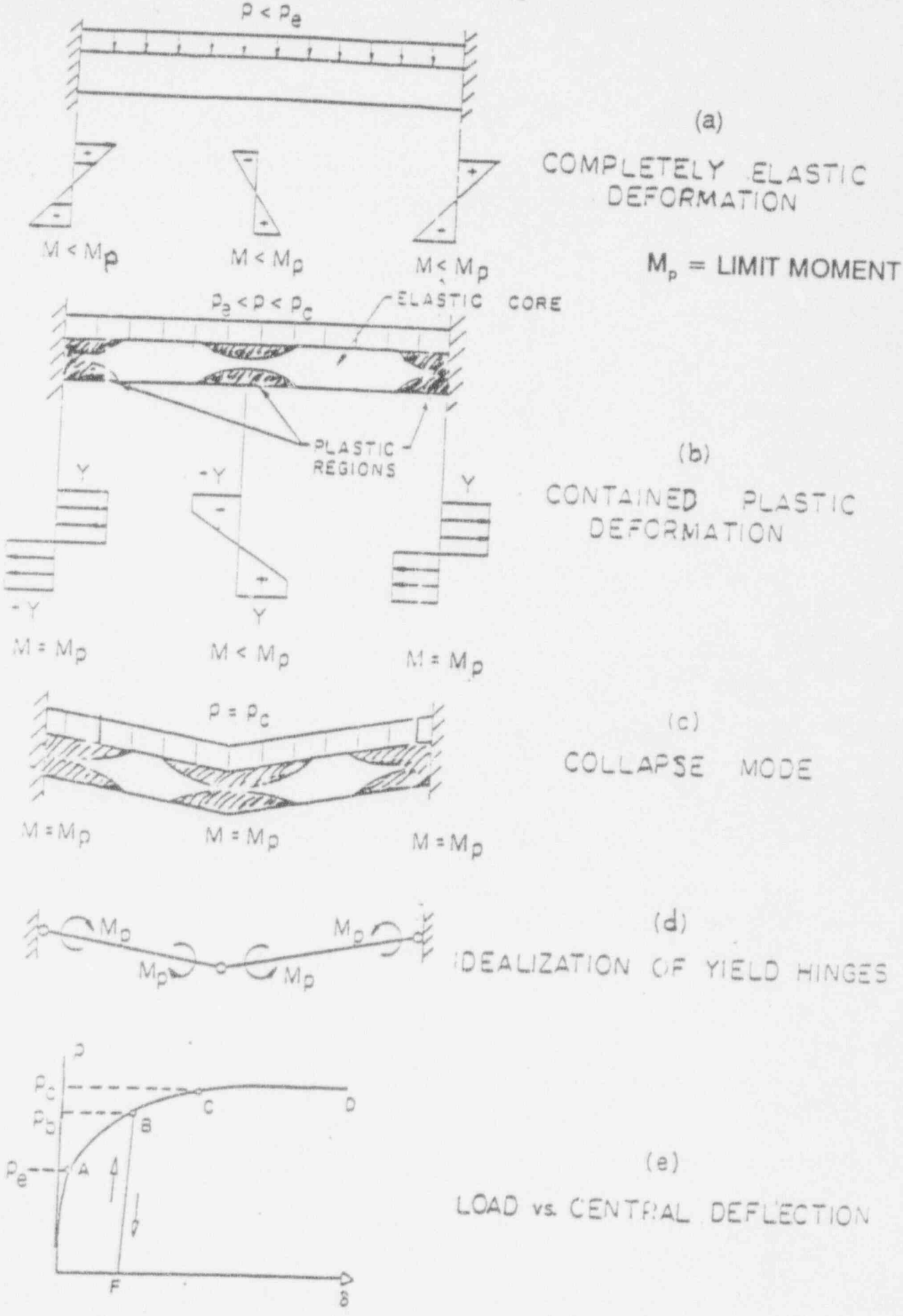

FIGURE 9 BEAM LOADING